

Reflective scattering at the LHC and two-scale structure of a proton

S.M. Troshin, N.E. Tyurin

*NRC “Kurchatov Institute”–IHEP
Protvino, 142281, Russian Federation,
Sergey.Troshin@ihep.ru*

Abstract

We discuss interpretation of the reflective scattering mode connecting its appearance with a resolution of a two-scale structure of a proton revealed in the DVCS process at Jefferson laboratory and in the differential cross-section of elastic pp -scattering at the LHC at the energy of $\sqrt{s} = 13$ TeV.

Introduction. The reflective scattering mode

As it is well known, the elastic scattering matrix element can be represented in a general form as the complex function:

$$S(s, b) = \kappa(s, b) \exp[2i\delta(s, b)] \quad (1)$$

with the two real functions κ and δ and κ can vary in the interval $0 \leq \kappa \leq 1$. The impact parameter b , $b = 2l/\sqrt{s}$, is a conserved quantity at high energies. The function κ is known as an absorption factor, its value $\kappa = 0$ means a complete absorption of the initial state, it is related to the probability distribution of the inelastic interactions over impact parameter:

$$\kappa^2(s, b) = 1 - 4h_{inel}(s, b), \quad (2)$$

where $h_{inel}(s, b)$ is a total contribution of the inelastic intermediate states into the unitarity relation:

$$\text{Im}f(s, b) = |f(s, b)|^2 + h_{inel}(s, b). \quad (3)$$

Note that the normalization is such that $S = 1 + 2if$, where f is the scattering amplitude. Unitarity relation in the impact parameter representation implies that the limiting behaviour $\text{Im}f \rightarrow 1$ leads to a vanishing real part of scattering amplitude, i.e. $\text{Re}f \rightarrow 0$, cf. [1].

It was shown in [2, 3] that the inelastic overlap function h_{inel} values are very close to its limiting value (in the present normalisation it is $h_{inel}^{max} = 1/4$) in the rather broad region of impact parameters, i.e. till $b \simeq 0.4$ fm at the LHC energy $\sqrt{s} = 13$ TeV. Deviation of h_{inel} from the maximal value is small and negative in this region of impact parameters (note, that $h_{inel}(s, b)$ has a shallow local minimum at $b = 0$). Then the unitarity relation at this energy and impact parameters can be written as

$$(\text{Im}f - 1/2)^2 + (\text{Re}f)^2 \simeq 0. \quad (4)$$

It follows from Eq. (4) that $\text{Re}f \simeq 0$ and $\text{Im}f \simeq 1/2$. Thus, the observed impact parameter picture of elastic scattering together with unitarity can provide at least a qualitative explanation of the recent result on the unexpectedly small real to imaginary parts ratio of the forward scattering amplitude [4]. Indeed, the above region of impact parameters being a most significant one provides leading contributions to the real and imaginary parts of a forward scattering amplitude¹. There is no room for a significant value of the real part of elastic scattering amplitude at $\sqrt{s} = 13$ TeV. Therefore, the real part of the elastic scattering amplitude f can be safely neglected due to its smallness (cf. for the numerical estimations [5],

¹Those parts are the respective integrals of the functions $\text{Re}f$ and $\text{Im}f$ over impact parameter.

qualitative arguments have been given above). And the following simplifying replacement will be used: $f \rightarrow if$.

The function $S(s, b)$ can be a nonnegative one in the whole region of the impact parameter variation or it can acquire negative values in the region $b < r(s)$ at high enough energy, i.e. at $s > s_r$, where s_r is a solution of the equation $S(s, b = 0) = 0$ (note that $r(s)$ is defined as $S(s, b = r(s)) = 0$ at $s > s_r$). The s -dependent function $r(s)$ increases as $\ln s$ at $s \rightarrow \infty$ [7] and its value at $\sqrt{s} = 13$ TeV is about 0.4 fm. This is the region of energies where the reflection appears, i.e. the function $S(s, b)$ crosses zero at $b = r(s)$ and the value of δ jumps from 0 to $\delta = \pi/2$ at this point. Since reflective scattering is not a commonly accepted nomenclature nowadays, a brief reminder of the main features of this mode is necessary.

Under the reflective scattering, $f > 1/2$, an increase of elastic scattering amplitude f correlates with decrease of h_{inel} according to unitarity relation

$$(f - 1/2)^2 = 1/4 - h_{inel} = \kappa^2/4 \quad (5)$$

and the term antishadowing has initially been used [6] emphasizing that the reflective scattering is correlated with the self-damping of the inelastic channels contribution [8] and decoupling of the elastic scattering from multiparticle production dynamics with energy increase. This phenomena is referred nowadays as hollowness [9–12].

The negative values of $S(s, b)$ correspond to the value of $\delta = \pi/2$. The term reflective has been borrowed from optics where phases of incoming and outgoing waves differ by π . Such phase jump takes place when the reflecting medium gets higher optical density (i.e. it has a higher refractive index) than the medium where incoming wave comes from. Optical density is then energy-dependent function. Here there is an analogy with the sign change of the electromagnetic wave under its reflection by the surface of a conductor. The energy evolution of the effective scatterer leads to appearance of the reflective scattering mode (provided the unitarity saturation takes place in the limit of $s \rightarrow \infty$).

Reflective scattering mode does not imply any kind of hadron transparency in the head-on collisions. Rather, it is about the geometrical elasticity [13]. The term transparency is relevant for the energy and impact parameter range related to the shadow scattering regime only, i.e. where $f < 1/2$. The interpretation of the reflective scattering mode which is based on the consideration of inelastic overlap function alone is, therefore, a deficient one, it does not provide any information on the collision elasticity.

The emerging physical picture of high energy hadron interaction region in transverse plane can be visualized then in the form of a reflective disk (with its albedo approaching to complete reflection at the center) which is surrounded by

a black ring (with complete absorption, $h_{inel} = 1/4$) since the inelastic overlap function h_{inel} has a prominent peripheral form at $s \rightarrow \infty$ in this scattering mode. The reflection mode implies that the following limiting behavior²

$$S(s, b)|_{b=0} \rightarrow -1 \quad (6)$$

will take place at $s \rightarrow \infty$ due to self-damping of the contributions of the inelastic channels [8]. Asymptotic growth of the total cross-section corresponds to saturation of unitarity and comes from an energy increase of the reflective disk radius and its albedo. Inelastic processes give a subleading contribution at $s \rightarrow \infty$.

Of course, it is considered that a monotonic increase of the amplitude f with energy to its unitarity limit $f = 1$ takes place, and an unrealistic option of its nonmonotonic energy dependence at fixed values of b is excluded.

QCD is a theory of hadron interactions with colored objects confined inside those entities. One can imagine that the color conducting medium is being formed instead of color insulating one when the energy of the colliding hadrons increases beyond some threshold value. Properties of such a medium are under active studies in nuclear collisions, but color conducting phase can be generated in hadron interactions too. Appearance of the reflective scattering mode can be associated with formation of the color conducting medium in the intermediate state of hadron interaction [16].

The two recent experiments at JLab and the LHC [17, 18] have proved to be significant and complementary for understanding the proton structure as well as the structure of the proton interactions region. Usage of the impact parameter picture and address to the reflective scattering mode allow combining analysis of the results from those experiments for physics interpretation of the reflective scattering.

1 Picture of a proton in soft processes

One can address the problem of the microscopic interpretation of the reflective scattering on the base of the new observations of the inner proton structure obtained in Jefferson Laboratory [17]. Those are in favor of the hypothesis of the dominance of elastic scattering in the deconfined mode.

An existence of a strong positive repulsive pressure has been detected at the center of the proton under investigations of its structure. The value of this repulsive pressure exceeds the one in the neutron stars [17]. The binding (negative)

²Despite the limiting behavior of $S(s, b)$ corresponds to $S \rightarrow -1$ at $s \rightarrow \infty$ and fixed b , the gap survival probability tends to zero at $s \rightarrow \infty$ and, in particular, contribution of the central production processes is consistent with unitarity contrary to conclusion of [14], see for details [15].

pressure exists in the peripheral part of the proton. One should note that such pressure distribution is a typical one for the chiral quark-soliton model [19, 20] where constituent quarks are confined due to interaction with a self-consistent pion field. Similar pressure distribution can also be expected in the models for hadron structure and their interactions proposed in [21–25].

In general, the soft hadron interactions are described by the nonperturbative sector of QCD. In this regime QCD should provide the two important phenomena: confinement (scale $\Lambda_{QCD} = 100 - 300$ MeV) and spontaneous breaking of chiral symmetry ($\Lambda_\chi \simeq 4\pi f_\pi \simeq 1$ GeV). Chiral symmetry is spontaneously broken between these two scales and this breaking generates quark masses. Since the soft hadron interactions occur at the distances where chiral symmetry is spontaneously broken one can conclude that a major role in such interactions belongs to constituent quarks [26] which are the colored but not pointlike objects. In addition to acquiring the masses, the strong interaction dynamics provides them with finite sizes, too. Chiral models describe baryon as consisting from an inner core with baryonic charge and an outer cloud surrounding the core. Interpretation of the results of the CLAS experiment at Jefferson Laboratory based on the existence of the extended substructures inside the proton was proposed in [27]. Presence of the inner repulsive core is in agreement with the recent direct DVCS data [17] and with the indirect LHC data at $\sqrt{s} = 13$ TeV [3, 18].

On the above basis one can assume that the different aspects of hadron dynamics are represented in the following form of the effective Lagrangian [28]:

$$\mathcal{L}_{eff} = \mathcal{L}_\chi + \mathcal{L}_I + \mathcal{L}_C, \quad (7)$$

where term \mathcal{L}_χ is responsible for providing constituent quarks the finite masses and sizes, \mathcal{L}_I describes their interaction mediated by the Goldstone bosons and \mathcal{L}_C — the color confinement. The latter term is switched off when the reflective scattering mode appears, it is switched off first in the central collisions (deconfinement) like it happens in the bag model [29]) and in this mode the geometric elastic scattering of hadron cores starts to appear and becomes noticeable. Thus, confining pressure begins to disappear in the high-energy central collision at $s > s_r$ and changes in the particle production mechanism would take place: maximal probability of the secondary particles production will take place in the peripheral collisions, $b \neq 0$.

2 Second diffraction cone in $d\sigma/dt$ as a result of the proton's cores interaction.

The second exponential slope [3, 18] observed in the differential cross-section behavior at the LHC at large values of $-t$ is in favor of the presence of a core in

the hadron structure and color deconfinement under collisions with small values of b . Indeed, due to deconfinement the scattering in the deep-elastic region becomes sensitive to presence of the inner core. Thus, one can consider the two exponential slopes observed in the differential cross-section at the LHC as a consequence of the two-component structure of a proton. The idea of a proton core is not new at all, it has been discussed by Orear in [30]. A core is a typical feature of various chiral models representing baryon as an inner core carrying baryonic charge and an outer cloud [31].

The outer cloud of the proton is responsible for confinement. The interactions of the proton's clouds are responsible for multiparticle reactions [32]. Those interactions lead to the first exponential cone observed at small transferred momenta in the elastic processes. This first cone appears as a result of unitarity relation connecting elastic and inelastic scatterings.

Note, however, that Orear type dependence of $d\sigma/dt$ in the region of $-t$ beyond the dip,

$$d\sigma/dt \sim \exp(-\tilde{b}_2\sqrt{-t}), \quad (8)$$

is in a good agreement with the data at moderate energies (CERN ISR data) in a rather wide range of $-t$ variation [33]. This dependence is considered usually as a result of a contribution of the branch points in the complex angular momentum plane generated by multiple rescatterings as a direct result of unitarity in the shadow scattering region where applicable [34–36].

It was shown in [37] that use of the functional dependence (8) at the LHC ($\sqrt{s} = 7$ TeV) fits the experimental data better than the power-like dependence and it was claimed that utilization of the power-like dependence is not preferable since a rather limited range of transferred momenta (till the value of $-t = 2.5$ (GeV/c)²) has been covered at $\sqrt{s} = 7$ TeV. However, such extension to the higher LHC energies in its turn has appeared to be again a not preferable one also due to a too narrow range (but not due to the collision energy value) of transferred momenta covered.

Currently, the data are available for the energy $\sqrt{s} = 13$ TeV [18]. Increase of the collision energy has allowed one to expand the range of transferred momenta available for the measurements up to $-t \simeq 4$ (GeV/c)². It has appeared now that exponential dependence on $-t$ fits the data significantly better than exponential dependence of $\sqrt{-t}$. Of course, this conclusion should be taken with caution since the range of available transferred momenta is not too wide again. At the moment we have no experimental data for $d\sigma/dt$ at the LHC energies in the range of $-t$ which was available for the measurements at the CERN ISR $\sqrt{s} = 53$ GeV. However, a good agreement of Philips–Barger parameterization of amplitude with the experimental data on $d\sigma/dt$ (cf. [38] and references therein) is in favor of the above conclusion on presence of the second cone in the differential cross-

section of elastic scattering. The slope parameter of the second cone is an energy-dependent one. It has a similar energy-dependence to the slope parameter of the first cone. This similarity, in particular, is implied by the scaling dependence of the rescaled differential cross-section of elastic pp -scattering at the LHC energies. This scaling has been discussed in [39].

We suggest that the observed deviation of $d\sigma/dt$ from the Orear dependence

$$\exp(-\tilde{b}_2\sqrt{-t}) \quad (9)$$

at the LHC is in favor of the functional dependence of $d\sigma/dt$ in the form of a linear exponent

$$\exp(-b_2t) \quad (10)$$

in the region of transferred momenta beyond the dip is a manifestation of a second scale in the hadron structure which in its turn is related to the reflective scattering mode. The magnitude of the ratio of the two scales sizes is correlated with the ratio of the first and second slopes values of $d\sigma/dt$ dependence on $-t$. These ratios can be approximately connected by the relation:

$$b_1/b_2 \simeq (r_p/r_c)^2, \quad (11)$$

where r_p is the proton radius and r_c is the radius of its core. From the experimental data at $\sqrt{s} = 13$ TeV one can approximate the value of a core radius as

$$r_c \simeq 0.5r_p$$

(cf. e.g. [40]).

Thus, the proton in soft processes resembles a hard ball coated with a thick but fragile shell. Energy evolution of the proton interactions can be imagined as follows. Interactions of the fragile shells (responsible for the inelastic processes) dominates up to the LHC region of energies and elastic scattering at those energies is just a shadow of the inelastic processes, while at the LHC the elastic scattering becomes sensitive to the core interactions in the central collisions (at $b \simeq 0$) first and acquires a pure geometrical component [41] due to high energy of collision. Interaction of the cores provides thus, in particular, a second exponential cone in $d\sigma/dt$ and the elastic interaction gradually acquires a geometric nature at small values of the impact parameter. Radius of the core interactions is correlated with the solution of equation

$$h_{el}(s, b) = 1/4, \quad (12)$$

at fixed energy $s > s_r$, where $h_{el}(s, b) = f^2(s, b)$ is the elastic overlap function. This solution is determined by dynamics of the peripheral clouds and the cores interaction.

As a result an increase of the ratio $\sigma_{el}(s)/\sigma_{tot}(s)$ [42] takes place due to redistribution of probabilities between elastic and inelastic interactions in favor of the elastic ones. This redistribution starts to appear in the region of small impact parameters and proliferates into the region of higher impact parameter values at higher energies. At the LHC energy $\sqrt{s} = 13$ TeV this region cover the range of impact parameters $0 \leq b \leq 0.4$ fm. The mechanism will lead to the elastic scattering dominance at $s \rightarrow \infty$, increasing with energy decoupling of elastic scattering from inelastic production processes [43] and respective slow down of the mean multiplicity growth at the LHC energies and beyond [44]. It gradually turning into a driver of the total cross-section growth at high energies.

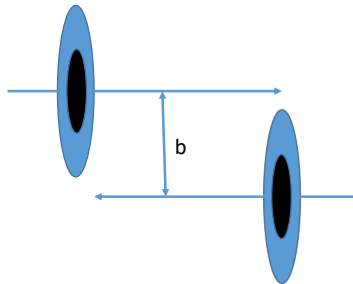


Figure 1: Two-components' protons scattering at the impact parameter b .

The form and size of the interaction region with reflective (geometric) scattering contribution in the impact parameter space are consistent with the impact parameter analyses at the LHC energy $\sqrt{s} = 13$ TeV [2,3]. As it was shown in [3], a statistical significance of the “black ring” effect at this energy is greater than 5σ , the real part of the scattering amplitude gives a very small contribution as it was expected and does not change the result. Thus, the existence of the “black ring” effect should be considered now as an experimentally established fact. As it was noted in [3] a dip at $b = 0$ becomes a generic property of the inelastic overlap function at high enough energies.

The appearance of the reflective scattering mode can be interpreted as a result of the color conducting phase formation at high energies. Therefore, presence of reflective scattering mode contribution emphasizes importance of the events classification according to the impact parameter of the collision since the reflective

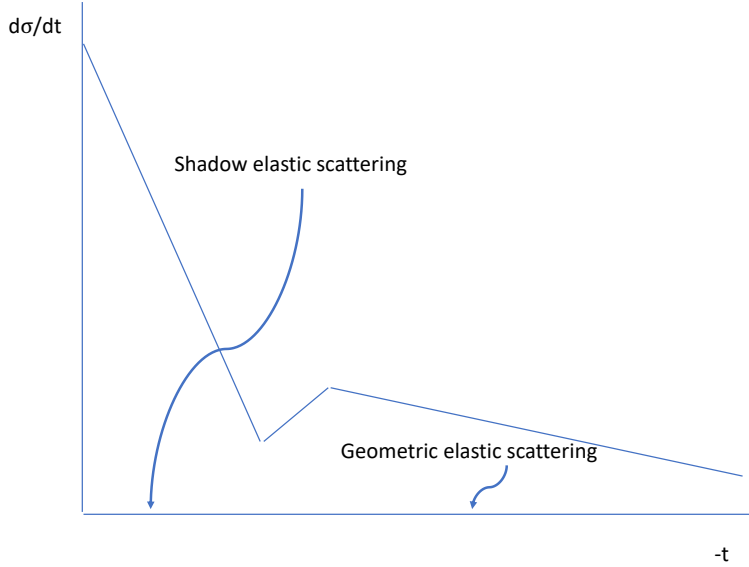


Figure 2: Two regions of transferred momenta $-t$ (relevant for shadow and geometric elastic scattering) in $d\sigma/dt$ at the LHC energies. The size of shadow scattering region diminishes with energy (decoupling of elastic scattering from multiparticle production) and tends to zero at $s \rightarrow \infty$.

scattering affects those with small impact parameters [45].

Thus, one can qualitatively conclude that behavior of the differential cross-section at the LHC energies follows a linear exponential dependence in both regions corresponding to the shadow scattering and to geometric scattering. Region of transferred momenta where the geometric scattering³ is dominating increases with energy and results in shift of the dip in the differential cross-section $d\sigma/dt$ into the region of smaller values of $-t$. The two regions are schematically represented at Fig. 2. Asymptotically, domination of geometric scattering would lead to saturation of unitarity limit, i.e. to a flat form of a scattering amplitude at small and moderate impact parameters which would result in typical diffraction pattern of the differential cross-section with many secondary maxima and minima [46] similar to the one observed in nuclei collisions [47].

It should be emphasized that the collision geometry describes the hadron interaction region but not the spacial properties of the individual participating hadrons. This geometry is determined by both a structure of interacting hadrons and dynamics of their interactions.

³Geometrical scattering gives, however, a rather small contribution to the integrated cross-section of elastic scattering $\sigma_{el}(s)$ at the LHC energies.

3 Conclusions

The general statement is that an expected transition from the shadow to geometric elastic scattering could start to occur already at the LHC energies. The claim is supported, in particular, by the interpretation of the second cone observed at the LHC as a consequence of a core in the hadron structure.

Dynamics of elastic pp -scattering is described by a function $F(s, t)$ (spin degrees of freedom of the colliding protons are neglected) of the two Mandelstam variables s and t , the latter variable is conjugated to the impact parameter b . As it was noted, any quantity integrated over b is not sensitive to details of its dependence and therefore it cannot provide an sufficient information for conclusions on the interaction dynamics.

On the base of b -dependent consideration of elastic and inelastic interactions there was proposed a connection of the reflective scattering mode with formation of color-conducting medium in the intermediate state at high energies and small impact parameter values [16]. This analogy is based on replacement of an electromagnetic field by a chromomagnetic field of QCD. One can also address the phenomenon of Andreev reflection at the boundary of the normal and superconducting phase [48, 49].

Presence of the core in a proton can be considered as a result of the different values of the scales Λ_{QCD} and Λ_χ relevant for the two important phenomena in the nonperturbative QCD: confinement and spontaneous chiral symmetry breaking. The latter phenomena seems to be relevant for a core formation. As it was noted before, the proton structure can be imagined as a hard ball placed in the hadron central region and coated by a fragile peripheral stuff. This hypotheses on core in a proton is relevant for the soft interactions, we do not concern here the hard ones where hadron's structure at the very short distance is important and where the parton model of hadrons with perturbative QCD are working well. The problem of transition between these two pictures is correlated with the problem of transition from \mathcal{L}_{QCD} to \mathcal{L}_{eff} . Above structure devoid an assumption⁴ of particle production the status of a leading driver of an asymptotic hadron interaction dynamics. The emergent substitution, i.e. hypothesis of maximal importance of elastic scattering, is based on the saturation of unitarity due to a maximal strength of strong interactions (i.e. maximality of the imaginary part of the partial amplitude of elastic scattering consistent with unitarity constraint). This principle has been developed by Chew and Frautchi along with the "strip approximation" [51].

No doubt, future experimental measurements would be crucial for the studies of hadron dynamics in the nonperturbative sector of QCD and allow one, in

⁴This assumption corresponds to the black limit saturation at $s \rightarrow \infty$, cf. e.g. [50], with equipartition of the elastic and inelastic cross-sections in this limit.

particular, to perform a sensible choice among shadow and geometric elastic scattering hypotheses, i.e. between the principles of maximal importance of particle production and maximal strength of strong interactions in the limit $s \rightarrow \infty$.

Acknowledgements

We are grateful to T. Csörgő for the interesting and useful correspondence on the two-scale structure of a proton in the context of the recent data of the LHC on the differential cross-section of elastic scattering at $\sqrt{s} = 13$ TeV.

References

- [1] S.M. Troshin, Phys. Lett. B **682**, 40 (2009).
- [2] A. Alkin et al., arXiv: 1807.06471v2.
- [3] T. Csörgő, R. Pasechnik, A. Ster, arXiv:1910.08817.
- [4] G. Antchev et al. (TOTEM Collaboration), Eur. Phys. J. C **79**, 785 (2019).
- [5] I.M. Dremin, V.A. Nechitailo, S.N. White, Eur. Phys. J. C **77**, 910 (2017).
- [6] S.M. Troshin, N.E. Tyurin, Phys. Lett. B **316**, 175 (1993).
- [7] S.M. Troshin, N.E. Tyurin, Int. J. Mod. Phys. A **22** 4437 (2007) .
- [8] M. Baker, R. Blankenbecler, Phys. Rev. **128**, 415 (1962).
- [9] W. Broniowski et al. Phys. Rev. D **98**, 074012 (2018).
- [10] E. Ruiz Arriola, W. Broniowski, Phys. Rev. D **95**, 074030 (2017).
- [11] J. L. Albacete, A. Soto-Ontoso, Phys. Lett. B **770**, 149 (2017).
- [12] J.L. Albacete, H. Petersen, A. Soto-Ontoso, Phys.Rev. C **95**, 064909 (2017).
- [13] S.M. Troshin, N.E. Tyurin, Phys. Rev. D **88**, 077502 (2013).
- [14] V.A. Khoze, A.D. Martin, M.G. Ryskin, Phys. Lett. B **780**, 352 (2018).
- [15] S.M. Troshin, N.E. Tyurin, Mod. Phys. Lett. A **23** , 169 (2008).
- [16] S.M. Troshin, N.E. Tyurin, J. Phys. G: Nucl. Part. Phys. **46**, 105009 (2019).
- [17] V.D. Burkert, L. Elouadrhiri, F.X. Girod, Nature **557**, 396 (2018).
- [18] G. Antchev et al. (TOTEM Collaboration) Eur. Phys. J C **79**, 861 (2019).

- [19] K. Goeke et al. Phys. Rev. D **75**, 094021 (2007).
- [20] M. Wakamatsu, Phys. Rev. D **46**, 3762 (1992).
- [21] M.M. Islam, Z. Phys. C **53**, 253 (1992).
- [22] L.L. Jenkovszky et al., Int. J. Mod. Phys. A **25**, 5667 (2010).
- [23] S.V. Goloskokov, S.P. Kuleshov, O.V. Selyugin, Sov. J. Nucl. Phys. **35**, 895 (1982).
- [24] S.M. Troshin, N.E. Tyurin, Phys. Rev. D **49**, 4427 (1994).
- [25] J. Pumplin, G.L. Kane, Phys. Rev. D **11**, 1183 (1975).
- [26] I.I. Royzen, E.L. Feinberg, O.D. Chernavskaya, Phys. Uspekhi **47**, 427 (2004).
- [27] R. Petronzio, S. Simula, G. Ricco, Phys. Rev. D **67**, 094004 (2003).
- [28] T. Goldman, R.W. Haymaker, Phys. Rev. D **24**, 724 (1981).
- [29] F.E. Low, Phys. Rev. D **12**, 163 (1975).
- [30] J. Orear, Phys. Rev. D **18**, 2484 (1978).
- [31] G.W. Heines, M.M. Islam, Nuov. Cim. **61**, 149 (1981).
- [32] I.M. Dremin, D.S. Chernavsky, Sov. Phys. JETP **11**, 167 (1960).
- [33] S.M. Troshin, N.E. Tyurin, Fiz. Elem. Chast. Atom. Yadra **15**, 53 (1984).
- [34] A.A. Anselm, I.T. Dyatlov, Phys. Lett. B **24**, 479 (1967).
- [35] I.V. Andreev, I.M. Dremin, JETP Lett. **6**, 262 (1967).
- [36] V.I. Savrin, N.E. Tyurin, O.A. Khrustalev, Yad. Fiz. **10**, 856 (1969).
- [37] S.M. Troshin, N.E. Tyurin, Mod. Phys. Lett. A **27**, 1250111 (2012).
- [38] V.P. Gonçalves, P.V.R.G. Silva, Eur. Phys. J. C **79**, 327 (2019).
- [39] T. Csörgő et al., arXiv:1912.11968.
- [40] I.M. Dremin, MDPI Particles **2**, 57 (2019).
- [41] S.M. Troshin, N.E. Tyurin, Phys. Rev. D **88**, 077503 (2013).
- [42] S.M. Troshin, N.E. Tyurin, Mod. Phys. Lett. A **33**, 1950259 (2019).
- [43] S.M. Troshin, N.E. Tyurin, Phys. Lett. B **707**, 558 (2012).
- [44] S.M. Troshin, N.E. Tyurin, Phys. Lett. B **732**, 95 (2014).
- [45] S.M. Troshin, N.E. Tyurin, Int. J. Mod. Phys. A **34**, 1950172 (2019).

- [46] S.M. Troshin, N.E. Tyurin, *Mod. Phys. Lett. A* **33**, 1850040 (2018).
- [47] M. Bleszynski, R.J. Glauber, P. Osland, *Phys. Lett. B* **104**, 389 (1981).
- [48] A.F. Andreev, *Sov. Phys. JETP* **19**, 1228 (1964).
- [49] M. Sadzikowski, M. Tachibana, *Acta Phys. Polon. B* **33**, 4141 (2002).
- [50] R. Gastmans, S.L. Wu, T.T. Wu, *Phys. Lett. B* **720**, 205 (2013).
- [51] G.F. Chew, S.C. Frautchi, *Phys. Rev. Lett.* **5**, 580 (1960).